ERRATUM: "A UNIVERSAL, LOCAL STAR FORMATION LAW IN GALACTIC CLOUDS, NEARBY GALAXIES, HIGH-REDSHIFT DISKS, AND STARBURSTS" (2012, ApJ, 745, 69)

Mark R. Krumholz[1], Avishai Dekel[2], and Christopher F. McKee[3]
[1] Department of Astronomy, University of California, Santa Cruz, CA 95064, USA; krumholz@ucolick.org
[2] Racah Institute of Physics, The Hebrew University, Jerusalem 91904, Israel; dekel@phys.huji.ac.il
[3] Departments of Physics and Astronomy, University of California, Berkeley, CA 94720, USA; cmckee@astro.berkeley.edu
Received 2013 October 11; published 2013 November 26

Online-only material: color figures

The published version of this paper contained three errors related to the data presented in Tables 3 and 4. First, due to a coding error, the object names are incorrect for some of the galaxies in Table 3. This did not affect the data themselves, only the labels assigned in the table. Second, again due a coding error, some of the computed free-fall times given in Table 4 were off by a factor of $\sqrt{\pi}$. The third was an incorrect entry for VIIZw 31 in Table 3; this goes back to an error in Daddi et al. (2010b), which was propagated into this paper.

Below we give corrected versions of Tables 3 and 4 from the published paper, a corrected version of Table 1 giving new best-fit parameters calculated from the corrected data, and new versions of the figures showing the corrected data. None of the conclusions of the paper are affected by these changes. In particular, correcting these errors changes the best-fit value for $\epsilon_{\rm ff}$ in the relation $\dot{\Sigma}_* = \epsilon_{\rm ff}(\Sigma/t_{\rm ff})$ from 0.010 to 0.015, while reducing the scatter from a factor of 2.8 to a factor of 2.7.

Table 1
Best Fit Parameters

Data Included in Fit	η	q	Scatter[a]
Fits to Figure 1, functional form[b] $\dot{\Sigma}_* = \eta\Sigma^q$			
Unresolved extragalactic disks	0.00019	1.31	2.2
Unresolved extragalactic starbursts	0.0028	1.26	2.3
All data	0.012	0.78	18
Fits to Figure 2, functional form[b] $\dot{\Sigma}_* = \eta(\Sigma/t_{\rm orb})^q$			
All unresolved extragalactic	0.23	1.13	2.7
All unresolved extragalactic, $q=1$	0.23	1.1	2.9
All	0.50	0.50	19
Fits to Figure 3, functional form $\dot{\Sigma}_* = \eta(\Sigma/t_{\rm ff})$			
All	0.015	$\cdots$	2.7

Notes.
[a] The scatter given is a multiplicative factor, so a scatter of unity indicates perfect agreement between data and fit.
[b] In these fits $\dot{\Sigma}_*$ has units of $M_\odot\,{\rm pc}^{-2}\,{\rm Myr}^{-1}$, Σ has units of $M_\odot\,{\rm pc}^{-2}$, and $t_{\rm orb}$ has units of Myr.

Table 3
Unresolved Local Extragalactic Data Set

Object	D/SB[a]	$\log\Sigma$ $(M_\odot\,{\rm pc}^{-2})$	$\log t_{\rm orb}$ (Myr)	$\log\Sigma/t_{\rm orb}$ $(M_\odot\,{\rm pc}^{-2}\,{\rm Myr}^{-1})$	$\log\dot{\Sigma}_*$ $(M_\odot\,{\rm pc}^{-2}\,{\rm Myr}^{-1})$	$\log t_{\rm ff,GMC}$[b] (Myr)	$\log t_{\rm ff,T}$[c] (Myr)	$\log\Sigma/t_{\rm ff}$[d] $(M_\odot\,{\rm pc}^{-2}\,{\rm Myr}^{-1})$	$100\epsilon_{\rm ff}$[e]
NGC 253	SB	2.60	1.18	1.42	1.00	1.63	−0.28	2.88	1.32
NGC 660	SB	1.85	1.66	0.19	−0.18	1.82	0.21	1.64	1.50
NGC 828	SB	2.91	1.41	1.50	0.86	1.55	−0.04	2.95	0.81
NGC 891	SB	1.86	1.34	0.52	−0.82	1.82	−0.11	1.97	0.16
NGC 1097	SB	1.92	1.46	0.46	−0.44	1.80	0.01	1.91	0.44
NGC 1614	SB	2.97	1.28	1.69	1.55	1.54	−0.17	3.14	2.53
NGC 1808	SB	1.90	1.72	0.18	−0.16	1.81	0.26	1.64	1.59
NGC 2146	SB	2.08	1.51	0.57	0.60	1.76	0.05	2.03	3.71
NGC 3034	SB	2.77	0.95	1.82	1.24	1.59	−0.50	3.27	0.93
NGC 3256	SB	2.38	2.09	0.29	0.44	1.69	0.63	1.75	4.91
NGC 3351	SB	2.08	1.11	0.97	−0.00	1.76	−0.34	2.42	0.38
NGC 3504	SB	2.15	1.30	0.85	−0.13	1.74	−0.15	2.30	0.37
NGC 3627	SB	1.53	1.58	−0.05	−1.01	1.90	0.13	1.40	0.38
NGC 4736	SB	1.50	1.15	0.35	−0.42	1.91	−0.31	1.81	0.59
NGC 5194	SB	1.74	1.64	0.10	−1.35	1.85	0.19	1.55	0.13
NGC 5236	SB	2.12	1.32	0.80	0.06	1.75	−0.13	2.25	0.64
NGC 6240	SB	3.36	1.38	1.98	1.63	1.44	−0.07	3.43	1.57

Table 3
(Continued)

Object	D/SB[a]	$\log \Sigma$ ($M_\odot$ pc^{-2})	$\log t_{\rm orb}$ (Myr)	$\log \Sigma/t_{\rm orb}$ ($M_\odot$ pc^{-2} Myr^{-1})	$\log \dot{\Sigma}_*$ ($M_\odot$ pc^{-2} Myr^{-1})	$\log t_{\rm ff,GMC}$[b] (Myr)	$\log t_{\rm ff,T}$[c] (Myr)	$\log \Sigma/t_{\rm ff}$[d] ($M_\odot$ pc^{-2} Myr^{-1})	$100\epsilon_{\rm ff}$[e]
NGC 6946	SB	1.51	1.97	−0.46	−0.54	1.90	0.52	0.99	2.93
IC 883	SB	3.20	1.36	1.84	1.30	1.48	−0.09	3.29	1.01
IC 1623	SB	3.06	1.38	1.68	1.43	1.52	−0.07	3.13	1.97
Maffei 2	SB	1.71	1.89	−0.18	−0.51	1.85	0.44	1.27	1.65
Arp 55	SB	1.98	2.13	−0.15	0.08	1.79	0.67	1.31	5.91
Arp 220	SB	4.01	0.78	3.23	2.74	1.28	−0.67	4.68	1.13
IR 10173+0828	SB	1.66	2.23	−0.57	0.24	1.87	0.77	0.89	22.37
VII Zw 31	SB	2.36	2.07	0.29	0.58	1.69	0.62	1.74	6.86
ZW 049	SB	3.15	1.28	1.87	1.53	1.49	−0.17	3.32	1.60
NGC 224	D	0.68	2.66	−1.98	−3.37	1.41	1.36	−0.68	0.20
NGC 598	D	1.03	2.60	−1.57	−2.71	1.33	1.30	−0.27	0.36
NGC 772	D	0.94	2.90	−1.96	−3.08	1.35	1.60	−0.41	0.21
NGC 925	D	0.91	2.86	−1.95	−2.68	1.36	1.56	−0.45	0.58
NGC 1569	D	1.33	2.30	−0.97	−1.04	1.25	1.00	0.33	4.23
NGC 2336	D	0.91	2.87	−1.96	−2.16	1.36	1.57	−0.45	1.92
NGC 2403	D	0.88	2.54	−1.66	−2.39	1.36	1.24	−0.36	0.93
NGC 2841	D	0.97	2.20	−1.23	−3.23	1.34	0.90	0.07	0.05
NGC 2903	D	0.86	2.49	−1.63	−2.55	1.37	1.19	−0.33	0.60
NGC 2976	D	0.98	2.11	−1.13	−1.90	1.34	0.81	0.17	0.85
NGC 3031	D	0.85	2.43	−1.58	−2.74	1.37	1.13	−0.28	0.34
NGC 3310	D	1.14	2.40	−1.26	−1.38	1.30	1.10	0.04	3.74
NGC 3338	D	0.81	2.60	−1.79	−2.80	1.38	1.30	−0.49	0.49
NGC 3368	D	0.93	2.43	−1.50	−2.79	1.35	1.13	−0.20	0.25
NGC 3486	D	0.88	2.51	−1.63	−2.70	1.36	1.20	−0.32	0.42
NGC 3521	D	1.22	2.52	−1.30	−2.15	1.28	1.22	0.00	0.70
NGC 3631	D	1.16	2.69	−1.53	−1.97	1.29	1.39	−0.13	1.45
NGC 3675	D	0.99	2.34	−1.35	−2.25	1.34	1.04	−0.05	0.63
NGC 3726	D	1.06	2.51	−1.45	−2.52	1.32	1.20	−0.14	0.42
NGC 3893	D	1.06	2.48	−1.42	−2.20	1.32	1.17	−0.11	0.82
NGC 4178	D	1.13	2.59	−1.46	−2.51	1.30	1.29	−0.16	0.44
NGC 4254	D	1.39	2.54	−1.15	−1.94	1.24	1.24	0.15	0.80
NGC 4258	D	0.59	2.68	−2.09	−2.60	1.44	1.38	−0.79	1.53
NGC 4294	D	1.02	2.48	−1.46	−2.11	1.33	1.17	−0.15	1.10
NGC 4303	D	1.21	2.68	−1.47	−1.98	1.28	1.38	−0.07	1.22
NGC 4321	D	1.14	2.65	−1.51	−2.31	1.30	1.35	−0.16	0.70
NGC 4394	D	0.63	2.51	−1.88	−3.12	1.43	1.20	−0.57	0.28
NGC 4402	D	1.08	2.62	−1.54	−3.04	1.31	1.32	−0.23	0.15
NGC 4501	D	1.09	2.52	−1.43	−2.45	1.31	1.22	−0.13	0.47
NGC 4519	D	0.99	2.46	−1.47	−2.22	1.34	1.16	−0.17	0.89
NGC 4535	D	1.01	2.72	−1.71	−2.62	1.33	1.41	−0.32	0.50
NGC 4548	D	0.69	2.53	−1.84	−2.76	1.41	1.23	−0.54	0.60
NGC 4561	D	1.52	2.20	−0.68	−2.17	1.20	0.90	0.62	0.16
NGC 4569	D	0.61	2.70	−2.09	−3.02	1.43	1.40	−0.79	0.58
NGC 4571	D	0.83	2.67	−1.84	−2.80	1.38	1.37	−0.54	0.55
NGC 4579	D	0.81	2.45	−1.64	−2.56	1.38	1.14	−0.33	0.59
NGC 4639	D	0.73	2.34	−1.61	−2.35	1.40	1.04	−0.31	0.91
NGC 4647	D	1.04	2.54	−1.50	−2.46	1.32	1.24	−0.20	0.55
NGC 4651	D	1.06	2.43	−1.37	−2.22	1.32	1.13	−0.07	0.70
NGC 4654	D	1.10	2.54	−1.44	−2.30	1.31	1.24	−0.14	0.69
NGC 4689	D	0.94	2.51	−1.57	−2.62	1.35	1.20	−0.26	0.44
NGC 4698	D	0.25	2.40	−2.15	−3.79	1.52	1.10	−0.85	0.11
NGC 4713	D	1.04	2.51	−1.47	−1.77	1.32	1.20	−0.16	2.45
NGC 4736	D	0.65	2.43	−1.78	−2.46	1.42	1.13	−0.48	1.04
NGC 5033	D	0.93	2.89	−1.96	−2.88	1.35	1.58	−0.42	0.34
NGC 5055	D	1.17	2.58	−1.41	−2.56	1.29	1.28	−0.11	0.35
NGC 5194	D	1.47	2.53	−1.06	−2.02	1.22	1.23	0.25	0.53
NGC 5236	D	1.70	2.45	−0.75	−1.65	1.16	1.14	0.56	0.62
NGC 5457	D	1.09	2.94	−1.85	−2.70	1.31	1.64	−0.22	0.33
NGC 6207	D	1.03	2.41	−1.38	−1.94	1.33	1.11	−0.08	1.38
NGC 6217	D	1.29	2.46	−1.17	−2.15	1.26	1.16	0.13	0.52
NGC 6503	D	0.89	2.23	−1.34	−2.32	1.36	0.93	−0.04	0.52
NGC 6643	D	1.11	2.57	−1.46	−2.05	1.31	1.27	−0.16	1.27
NGC 6946	D	1.30	2.54	−1.24	−2.12	1.26	1.24	0.06	0.66
NGC 7331	D	1.08	2.76	−1.68	−2.57	1.31	1.46	−0.23	0.46

Notes. All data are taken from Kennicutt (1998), adjusted to the same IMF and CO X factor as the high-z data following Daddi et al. (2010b).

[a] D: disk; SB: starburst.

[b] Computed from Equation (4) of the published paper using $\sigma = 8$ km s^{-1} for disks and $\sigma = 50$ km s^{-1} for starbursts.

[c] Computed from Equation (8) of the published paper using $Q = 1$, $\beta = 0$ for disks and $Q = 1$, $\beta = 1$ for starbursts.

[d] Computed using $t_{\rm ff} = \min(t_{\rm ff,GMC}, t_{\rm ff,T})$.

[e] Computed from $\epsilon_{\rm ff} = \dot{\Sigma}_*/(\Sigma/\min(t_{\rm ff,GMC}, t_{\rm ff,T}))$.

Table 4
Unresolved High-z Extragalactic Data Set

Object[a]	D/SB[b]	$\log \Sigma$ ($M_\odot$ pc^{-2})	$\log t_{\mathrm{orb}}$ (Myr)	$\log \Sigma/t_{\mathrm{orb}}$ ($M_\odot$ pc^{-2} Myr^{-1})	$\log \dot{\Sigma}_*$ ($M_\odot$ pc^{-2} Myr^{-1})	$\log t_{\mathrm{ff,GMC}}$[c] (Myr)	$\log t_{\mathrm{ff,T}}$[d] (Myr)	$\log \Sigma/t_{\mathrm{ff}}$[e] ($M_\odot$ pc^{-2} Myr^{-1})	$100\epsilon_{\mathrm{ff}}$[f]
Data from Genzel et al. (2010)
Q2343-MD59	D	2.74	2.34	0.40	−0.68	1.60	1.28	1.46	0.73
SMMJ02399−0136	SB	2.63	1.73	0.90	0.84	1.62	0.52	2.11	5.38
SMMJ09431+4700	SB	3.53	1.47	2.06	1.83	1.40	0.26	3.27	3.64
SMMJ105141+5719	SB	2.66	1.62	1.04	1.04	1.62	0.41	2.25	6.18
SMMJ123549+6215	SB	4.00	1.12	2.88	2.20	1.28	−0.09	4.09	1.29
SMMJ123634+6212	SB	2.58	1.87	0.71	0.63	1.64	0.66	1.92	5.14
SMMJ123707+6214	SB	2.73	1.74	0.99	1.01	1.60	0.53	2.20	6.47
SMMJ131201+4242	SB	2.99	1.63	1.36	1.09	1.53	0.42	2.57	3.32
SMMJ131232+4239	SB	3.18	1.56	1.62	1.29	1.49	0.35	2.83	2.89
SMMJ163650+4057	SB	3.42	1.46	1.96	1.37	1.43	0.25	3.17	1.59
Data from Bouché et al. (2007)
...	SB	2.90	1.80	1.10	1.10	1.56	0.59	2.31	6.22
...	SB	3.10	1.65	1.45	1.20	1.51	0.44	2.66	3.50
...	SB	3.25	1.80	1.45	1.15	1.47	0.59	2.66	3.12
...	SB	3.45	1.45	2.00	1.10	1.42	0.24	3.21	0.78
...	SB	2.30	1.55	0.75	1.40	1.71	0.34	1.96	27.80
...	SB	3.45	1.55	1.90	1.70	1.42	0.34	3.11	3.93
...	SB	3.30	1.50	1.80	1.80	1.46	0.29	3.01	6.22
...	SB	3.65	1.40	2.25	1.80	1.37	0.19	3.46	2.21
...	SB	3.35	1.25	2.10	2.00	1.44	0.04	3.31	4.94
...	SB	3.70	1.45	2.25	1.95	1.36	0.24	3.46	3.12
...	SB	3.20	1.55	1.65	2.10	1.48	0.34	2.86	17.54
...	SB	3.70	1.05	2.65	2.60	1.36	−0.16	3.86	5.55
...	SB	4.00	0.95	3.05	2.70	1.28	−0.26	4.26	2.78
Data from Daddi et al. (2010b)
...	D	2.39	2.08	0.31	−0.47	1.68	1.03	1.36	1.46
...	D	2.53	2.08	0.44	−0.36	1.65	1.03	1.50	1.38
...	D	1.75	2.08	−0.33	−1.27	1.84	1.03	0.72	1.01
Data from Daddi et al. (2010a)
BzK-4171	D	2.95	1.84	1.11	0.08	1.54	0.79	2.16	0.82
BzK-21000	D	2.96	1.62	1.34	0.19	1.54	0.57	2.39	0.63
BzK-16000	D	2.56	1.83	0.73	−0.03	1.64	0.78	1.78	1.56
BzK-17999	D	2.66	2.02	0.64	0.03	1.62	0.97	1.69	2.16
BzK-12591	D	2.53	2.15	0.38	−0.04	1.65	1.09	1.44	3.34
BzK-25536	D	2.88	2.25	0.63	0.05	1.56	1.20	1.68	2.32
Data from Tacconi et al. (2010)
EGS13004291	D	2.85	2.02	0.83	−0.28	1.57	0.97	1.88	0.69
EGS12007881	D	2.15	2.33	−0.17	−0.72	1.74	1.27	0.88	2.52
EGS13017614	D	2.46	2.03	0.43	−0.57	1.67	0.98	1.49	0.88
EGS13035123	D	2.30	2.28	0.01	−0.61	1.71	1.23	1.07	2.13
EGS13004661	D	1.87	2.21	−0.34	−0.52	1.82	1.15	0.72	5.78
EGS13003805	D	2.80	2.12	0.69	−0.25	1.58	1.07	1.74	1.03
EGS12011767	D	1.83	2.58	−0.75	−0.82	1.82	1.53	0.30	7.63
EGS12012083	D	2.44	2.33	0.11	−0.17	1.67	1.28	1.16	4.65
EGS13011439	D	2.07	2.12	−0.05	−0.62	1.76	1.07	1.00	2.39
HDF-BX1439	D	3.42	1.67	1.75	0.41	1.43	0.61	2.81	0.40
Q1623-BX599	D	2.19	2.28	−0.09	−0.60	1.73	1.22	0.97	2.74
Q1623-BX663	D	2.87	2.29	0.59	−0.18	1.56	1.23	1.64	1.52
Q1700-MD69	D	3.20	1.82	1.38	0.16	1.48	0.76	2.44	0.52
Q1700-MD94	D	2.01	2.09	−0.08	−0.66	1.78	1.04	0.97	2.35
Q1700-MD174	D	2.45	2.09	0.36	−0.49	1.67	1.04	1.41	1.27
Q1700-BX691	D	3.15	1.79	1.36	0.03	1.49	0.74	2.41	0.41

Notes.
[a] A blank entry indicates the object is not identified by name in the source reference.
[b] D: disk; SB: starburst.
[c] Computed from Equation (4) of the published paper using $\sigma = 8$ km s^{-1} for disks and $\sigma = 50$ km s^{-1} for starbursts.
[d] Computed from Equation (8) of the published paper using $Q = 1$, $\beta = 0$ for disks and $Q = 1$, $\beta = 1$ for starbursts.
[e] Computed using $t_{\mathrm{ff}} = \min(t_{\mathrm{ff,GMC}}, t_{\mathrm{ff,T}})$.
[f] Computed from $\epsilon_{\mathrm{ff}} = \dot{\Sigma}_*/(\Sigma/\min[t_{\mathrm{ff,GMC}}, t_{\mathrm{ff,T}}])$.
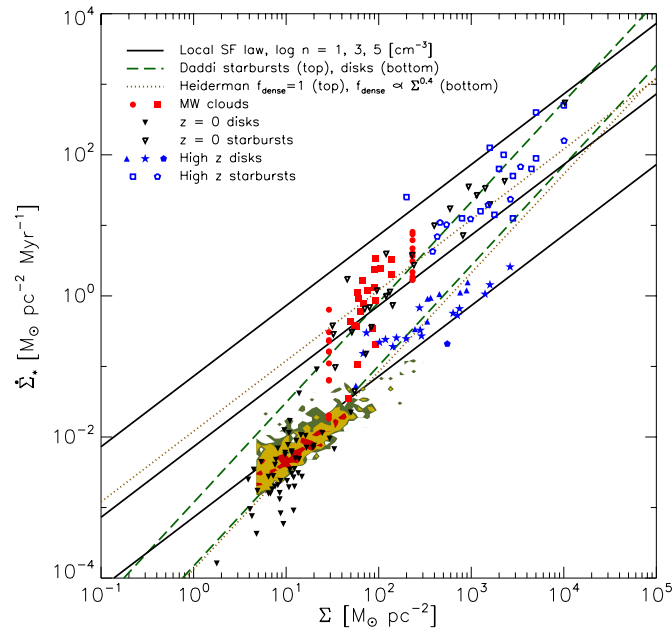
Figure 1. Corrected version of Figure 1 from the published paper. For details on the points, see the caption to the original figure.
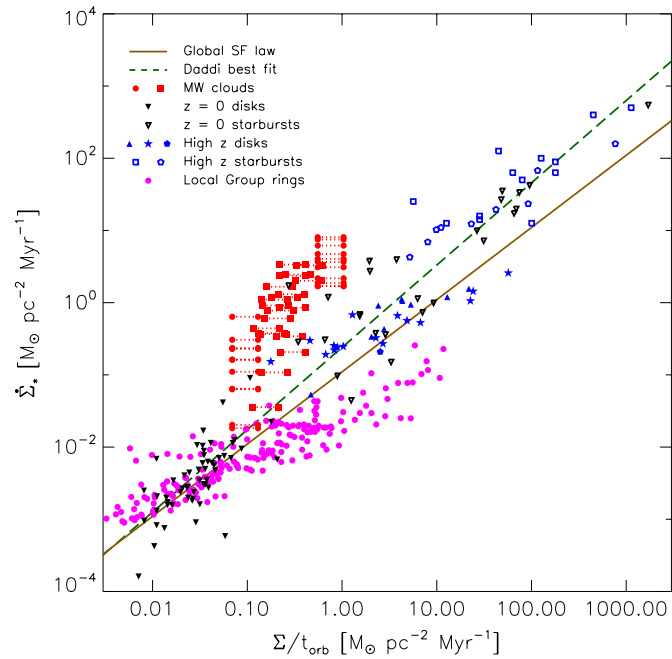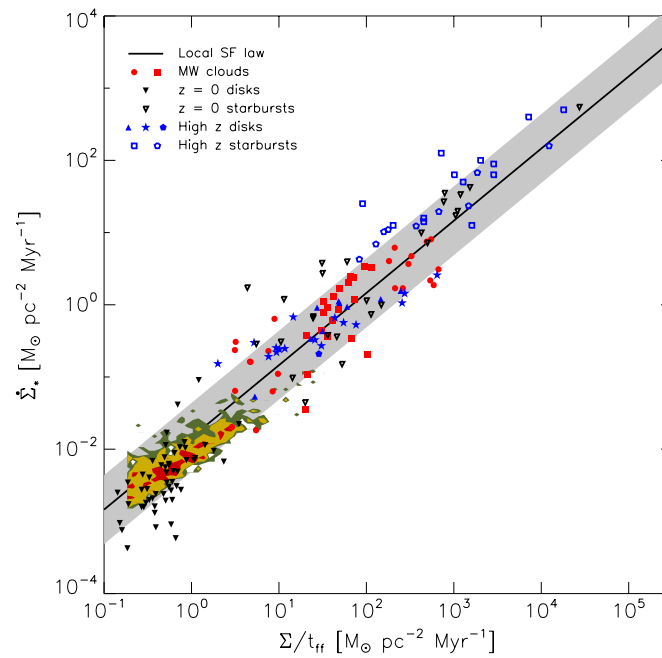(A color version of this figure is available in the online journal.)

Figure 2. Corrected version of Figure 2 from the published paper. For details on the points, see the caption to the original figure.
(A color version of this figure is available in the online journal.)
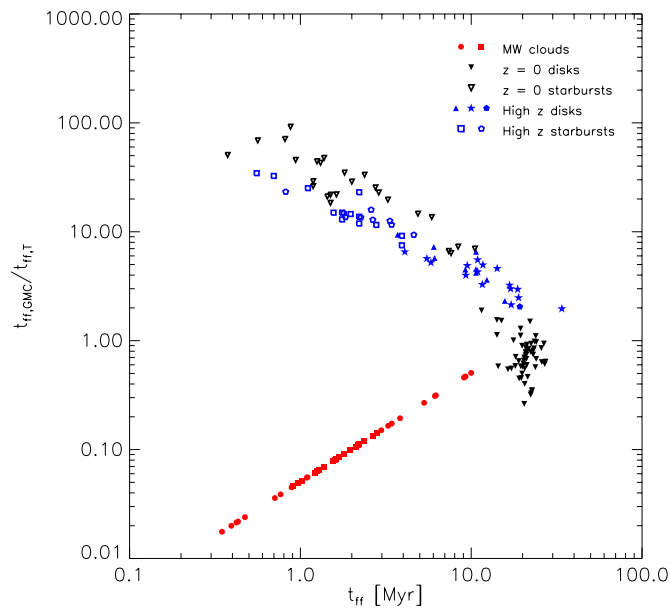
Figure 3. Corrected version of Figure 3 from the published paper. For details on the points, see the caption to the original figure.
(A color version of this figure is available in the online journal.)

Figure 4. Corrected version of Figure 4 from the published paper. For details on the points, see the caption to the original figure.
(A color version of this figure is available in the online journal.)

REFERENCES

Bouché, N., Cresci, G., Davies, R., et al. 2007, ApJ, 671, 303
Daddi, E., Bournaud, F., Walter, F., et al. 2010a, ApJ, 713, 686
Daddi, E., Elbaz, D., Walter, F., et al. 2010b, ApJL, 714, L118
Genzel, R., Tacconi, L. J., Gracia-Carpio, J., et al. 2010, MNRAS, 407, 2091
Kennicutt, R. C., Jr. 1998, ApJ, 498, 541
Tacconi, L. J., Genzel, R., Neri, R., et al. 2010, Natur, 463, 781